STABILITY ISSUES IN A CONTINUOUS LOOP REACTOR FOR FREE-RADICAL POLYMERIZATION

P. A. Melo[1], J.C. Pinto[1], E. C. Biscaia[1] and W. H. Ray[2]

[1]*PEQ/COPPE - Universidade Federal do Rio de Janeiro, Cidade Universitária,*
CP 68502, Rio de Janeiro, RJ – Brazil. E-mail: melo@peq.coppe.ufrj.br

[2]*Department of Chemical Engineering, University of Wisconsin,*
1415 Engineering Drive, Madison, WI 53706 - U.S.A.

Abstract: Continuous loop reactors are potential candidates for replacing stirred tanks in the free-radical polymer industry. Loop reactors present attractive advantages such as improved mixing and heat transfer capabilities and their macroscopic behavior is very close to the continuous stirred tanks. In this contribution, operability and stability issues associated to this equipment are studied. Simulation results are presented for the free-radical solution polymerization of vinyl acetate. It is shown that safe and stable reactor operation is strongly dependent on the proper choice of the process parameters. *Copyright © 2000 IFAC.*

Keywords: Stability Analysis, Modeling, Reactor, Polymerization.

1. INTRODUCTION

Most of the free-radical solution polymerization reactions in industry takes place in stirred tanks. The increase of the solution viscosity during the reaction and the low reactor area/volume ratio are limiting factors for mixing and heat transfer capabilities of these vessels. Tubular reactors seem to be natural alternative reactors for replacing the stirred tanks. The tubular geometry implies simplicity of reactor design and potential low cost. However, implementation of these vessels is slowed down by uncertainty about the polymer that would be produced (e.g. molecular weight distribution) and concerns about the operational difficulties (e.g. plugging, flow instabilities, etc) that might be encountered (Hamer, 1983).

In this scenario, loop reactors are industrially attractive because i) they are tubular (thus presenting an elevated area/volume ratio), and ii) they present the distribution of residence times of the stirred tanks, when operated at high internal flow rates. The reactor consists basically of a main tubular system closed in a loop. Both empty-tube and static-mixed-tube operation is possible. An axial pump provides the internal circulation flow and sets the rate of recirculation in the loop. High flow rates permit operation at high monomer conversions, thus representing an important advantage over the stirred tank where serious mixing and heat transfer limitations arise under these conditions.

Despite the relevant potential application of loop reactors in the free-radical polymerization industry, little is known about the operability and stability issues of this equipment. Fleury *et al.* (1992) designed a loop reactor for the free-radical solution polymerization of methyl methacrylate. Thermal instabilities were found experimentally in a static-mixed reactor. The auto-acceleration of the reaction due to the gel-effect was found to be the source of the instabilities. A plug-flow reactor model proved to be adequate for fitting their experimental data. Later on, Belkhiria et al. (1994) used this same apparatus to perform the copolymerization of styrene and maleic anhydride. It was shown that depending on the monomer in excess, the safe and stable operating conditions of the reactor may change.

No systematic study on the stability and dynamics of this reactor has been reported. In this contribution the modeling of a loop reactor for a free-radical process is presented. The reactor stability behavior is analyzed through dynamic simulations and parametric continuation procedures. The solution polymerization of vinyl acetate using methanol as solvent and AIBN as initiator is taken as a case study. An experimental apparatus has been set-up in order to verify the theoretical results presented here. These results will be reported elsewhere.

2. POLYMERIZATION KINETICS

The mathematical model used to describe the loop reactor in this work assumes the following free-radical polymerization mechanism:

Initiation

$$I \xrightarrow{k_d} 2R$$

$$R + M \xrightarrow{k_{pR}} P_1^{'}$$

Propagation

$$P_n + M \xrightarrow{k_p} P_{n+1}$$

$$P_n^{'} + M \xrightarrow{k_p} P_{n+1}^{'}$$

Termination by combination

$$P_n + P_m \xrightarrow{k_{TC}} M_{n+m}$$

$$P_n^{'} + P_m \xrightarrow{k_{TC}} M_{n+m}$$

$$P_n + P_m^{'} \xrightarrow{k_{TC}} M_{n+m}$$

$$P_n^{'} + P_m^{'} \xrightarrow{k_{TC}} M_{n+m}^{'}$$

Here I is the initiator, R is the free-radical species generated by decomposition of initiator, M is the monomer, S is the solvent or chain-transfer agent, P_i is the polymer molecule of length i, and M_i is the dead polymer molecule of length i. The prime denotes that the live or dead polymer molecule has a terminal double bond. The chain transfer to monomer, solvent, polymer and terminal double bond polymerization steps were omitted from the above mechanism for space reasoning. By applying the quasi-steady state approximation to live polymeric radicals, the expression for the total concentration of growing polymer molecules is derived as follows

$$[P] = \left(\frac{2fk_D I}{k_{TC}} \right)^{1/2} . \qquad (1)$$

Diffusional limitations at high polymer concentration are taken into account here by adopting a gel-effect correlation which assumes no temperature dependence. This is explained by the fact that moderate viscosities are encountered in solution polymerization. The gel-effect is given by

$$g_T = \exp(a_1 x_t + a_2 x_t^2 + a_3 x_t^3) . \qquad (2)$$

The parameters a_i (i=1,2,3) in Equation (2) were fitted by (Teymour, 1989) using vinyl acetate solution polymerization data. x_t is the monomer conversion based on total feed, including solvent.

3. REACTOR MODEL

The reactor modeling is performed by considering the reactor being composed of two distinct tubular zones, connected to each other by a mixing tank (Zacca, 1991). Figure 1 shows a sketch of this arrangement. Each tubular zone of the reactor is described according to the axial dispersion model. The inlet section is modeled as a perfect mixing tank with negligible capacitance.

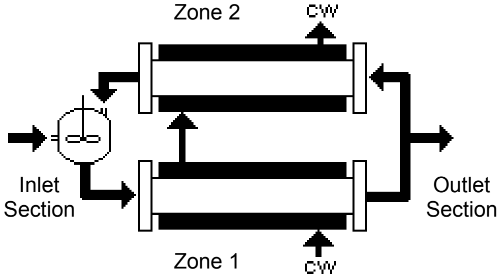

Fig. 1. Diagram of the loop reactor.

The dimensionless model equations are the following:

component mass balance in zone i (i=1,2)

$$\frac{\partial y^i(z,t)}{\partial t}+\frac{\partial y^i(z,t)}{\partial z}=\frac{1}{Pe_m^i}\frac{\partial^2 y^i(z,t)}{\partial z^2} - Da^i\cdot\Re_y^i \tag{3}$$

energy balance in zone i (i=1,2)

$$\frac{\partial \theta^i(z,t)}{\partial t}+\frac{\partial \theta^i(z,t)}{\partial z}=\frac{1}{Pe_h^i}\frac{\partial^2 \theta^i(z,t)}{\partial z^2} + B\cdot Da^i\cdot\Re_y^i+\beta^i(\theta_c-\theta) \tag{4}$$

where y represents the monomer, initiator, and solvent dimensionless concentrations, and θ represents the dimensionless reactor temperature. Two boundary conditions are required per tubular zone. In this work closed-closed boundary conditions have been chosen for both tubular zones

$$(1-\alpha)f_c+\alpha y^2(1,t)=y^1(0,t)-\frac{1}{Pe_m^1}\left.\frac{\partial y^1(z,t)}{\partial z}\right|_{z=0} \tag{5}$$

$$(1-\alpha)+\alpha\theta^2(1,t)=\theta^1(0,t)-\frac{1}{Pe_h^1}\left.\frac{\partial \theta^1(z,t)}{\partial z}\right|_{z=0} \tag{6}$$

$$\left.\frac{\partial y^1(z,t)}{\partial z}\right|_{z=1}=\left.\frac{\partial y^2(z,t)}{\partial z}\right|_{z=0} \tag{7}$$

$$\left.\frac{\partial \theta^1(z,t)}{\partial z}\right|_{z=1}=\left.\frac{\partial \theta^2(z,t)}{\partial z}\right|_{z=0} \tag{8}$$

$$y^1(1,t)=y^2(0,t) \tag{9}$$

$$\theta^1(1,t)=\theta^2(0,t) \tag{10}$$

$$\left.\frac{\partial y^2(z,t)}{\partial z}\right|_{z=1}=0 \tag{11}$$

$$\left.\frac{\partial \theta^2(z,t)}{\partial z}\right|_{z=1}=0 \tag{12}$$

where Rec is the recycle ratio, defined as the ratio of volumetric flow rates between the recycle stream and feed stream, as follows

$$Re\,c=\frac{Q_2}{Q_{Feed}}\,. \tag{13}$$

Continuity of the state variables and their corresponding fluxes has been assured through jump conditions expressed by Equations (7) to (10).

The reactor model consists of a set of partial differential equations and algebraic equations. By applying quadratic finite element approximation in the spatial direction according to the method of lines, the resulting system consists of a set of differential algebraic equations (DAE system). The integration of this DAE system in time was performed by means of the numerical integrator DDASSL (differential-algebraic system solver) (Petzold, 1982). Table 1 provides the simulation data used in this work.

Table 1 Reactor operational parameters

Definition	Value
Length of tubular sections	106.5 cm
Diameter of tubular sections	1.7272 cm
Coolant temperature	45°C
Heat of polymerization	21 kcal/gmol
Feed temperature	42°C
Feed monomer concentration	$7.34*10^{-3}$ gmol/cm^3
Feed solvent concentration	$7.34*10^{-3}$ gmol/cm^3
Feed initiator concentration	$3.80*10^{-5}$ gmol/cm^3

4. BIFURCATION ANALYSIS

In this section the methodology for the model bifurcation analysis is presented. It is well known that the stability of a given chemical process may change when some of its parameters undergo changes. Bifurcation theory provides analytical and numerical tools for evaluating the stability changes of mathematically modeled chemical processes. Essentially, parametric continuation techniques are applied to the process model in order to verify the existence of non-linear phenomena such as steady-state multiplicity and self-sustained oscillations.

The loop reactor model developed above originated a set of differential algebraic equations. This DAE system was implemented in the continuation package AUTO (Doedel *et al.*, 1997). AUTO code was modified in order to evaluate the stability of a DAE system. As shown by (Hyanek, 1995), a DAE system may be written in a implicit form according to

$$\mathbf{A}(\mathbf{x})\cdot\mathbf{x}'+\mathbf{f}(\mathbf{x},\mu)=\mathbf{0}\,. \tag{14}$$

Here **f** is a vector of non-linear functions, **x** and **x**' are the state variables and their time derivatives, and μ is some process parameter. **A**(**x**) represents a quadratic matrix function which is rank deficient. By linearizing Equation (14) around a steady-state ($\mathbf{x}=\mathbf{x}^*$) for a given value of parameter μ ($\mu=\mu_o$), the equation may be rewritten in the form

$$\mathbf{f}_\mathbf{x} \cdot \delta_\mathbf{x} + \mathbf{A}(\mathbf{x}) \cdot \delta_{\mathbf{x}'} = \mathbf{0} \qquad (15)$$

where the Jacobian $\mathbf{f}_\mathbf{x}$ and the matrix **A**(**x**) are evaluated at the steady-state of interest, $\delta_\mathbf{x}$ is a small perturbation about the steady-state and $\delta_{\mathbf{x}'} = \mathrm{d}(\delta_\mathbf{x})/\mathrm{dt}$. Equation (15) leads directly to a generalized linear characteristic value problem, which has to be solved during the continuation procedure of a modified version of AUTO.

5. RESULTS

The mixing pattern in a loop reactor may vary from the limiting case of a plug flow reactor (no mixing) to the continuous stirred tank reactor (complete mixing). The recycle ratio (which is given by the internal flow rate imposed) plays an important role on the reactor mixing. Figure 1 illustrates this issue by comparing the monomer conversion profiles in the reactor at different levels of recirculation. Higher recycle ratio imposes a better degree of mixing in the reactor, which can be observed by a flatter monomer conversion axial profile. A decrease in the outlet monomer conversion is expected since the reactor macrocospic behavior tends to that of the continuous stirred tank. Figure 3 illustrates a typical spatial-temporal steady-state approach in the reactor for low recycle ratios.

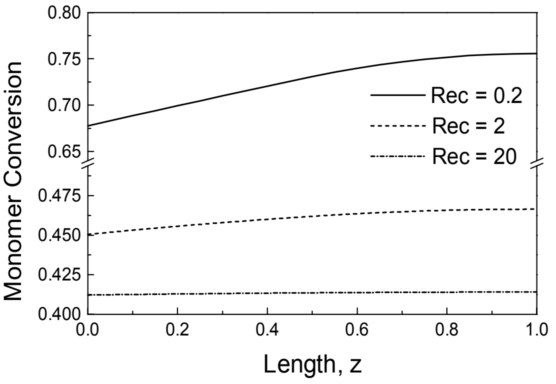

Fig. 2. Effect of the recycle ratio on the axial monomer concentration (τ=167min, U=7.0* 10^{-4} cal/cm^{2}s).

Reactor stability is now discussed. Residence time has been taken as the main continuation parameter for tracing out steady-state solutions branches. In this work, limit points and Hopf bifurcation points are the two elementary bifurcations considered. Figure 4 shows a typical bifurcation diagram for the loop reactor model developed above. A narrow range for steady-state multiplicity has been found, contrasting to a rather large range for self-sustained oscillations.

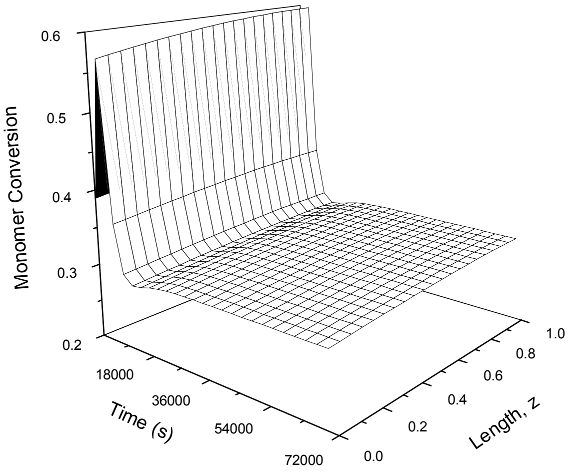

Fig. 3. Spatial-temporal monomer conversion profile in the loop reactor at low recycle ratio (Rec = 1.0, τ=167 min, U=7.0*10^{-4}cal/cm^{2}s).

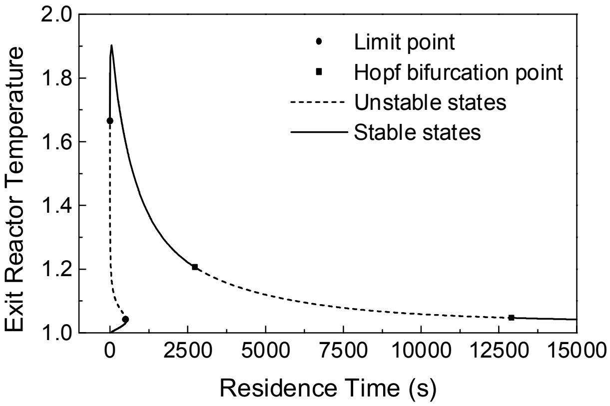

Fig. 4. Steady-state solutions branch for the reactor exit temperature (Rec=50, U=3.0*10^{-4} cal/cm^{2}s).

At lower recycle ratios the continuation diagrams are equivalent to the one shown above. However, a narrower ranges for self-sustained oscillations has been found, as illustrated in Figure 5. In Figure 5 the effect of the overall heat transfer coefficient on the bifurcation diagram may be also observed. Changes in this coefficient may lead to the onset of oscillatory behavior. Indeed, small perturbations in the overall heat transfer coefficients are responsible for the oscillations presented in Figure 6.

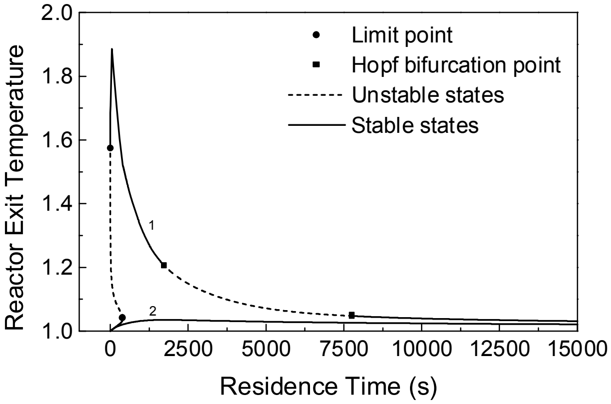

Fig. 5. Steady-state solutions branch for the reactor exit temperature with Rec=1.0; (1) U=3.0*10^{-4} cal/cm^{2}s, (2) U=5.0*10^{-4} cal/cm^{2}s.

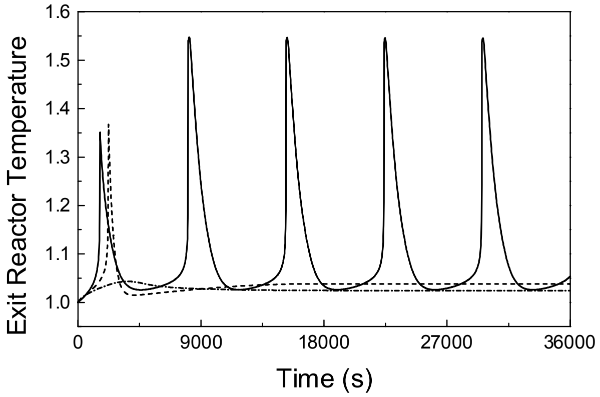

Fig. 6. Dynamic profiles of reactor exit temperatures (Rec=1.0, τ=167min, solid line U=3.0*10^{-4} cal/cm^{2}s, dashed line U=5.0*10^{-4} cal/cm^{2}s, dashed-dotted line U=7.0*10^{-4} cal/cm^{2}s).

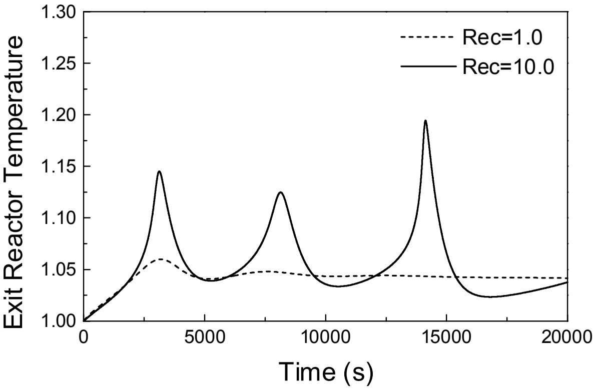

Fig. 7. Dynamic profiles of reactor exit temperatures (τ=167 min and U=3.0*10^{-4} cal/cm^{2}s).

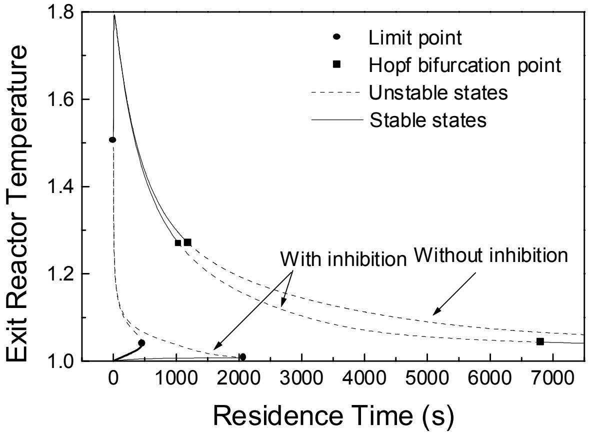

Fig. 8. Steady-state solutions branch for the reactor exit temperature with Rec=100; U=3.0*10^{-4} cal/cm^{2}s.

In Figure 7, induced self-sustained oscillations are observed after varying the recycle ratio. This behavior is apparently new for free-radical polymerization processes. In Figure 8, the effect of impurities in the system is considered by adding an inhibitor to the feed flow. As observed, the steady-state multiplicity range which is initially very narrow becomes wider and thus turns into a worrisome issue as far as process safety.

6. CONCLUSIONS

In this work theoretical results on stability of loop reactors applied in free-radical polymerization processes have been presented. The non-linear analysis of the reactor mathematical model has shown the reactor's high sensitivity to some operating parameters such as residence time, recycle ratio and overall heat transfer coefficient. It has been observed the induction of oscillatory behavior by varying the recycle ratio. Oscillations are also induced depending on the heat removal rates imposed on the reactor operation. The lower the overall heat transfer coefficient the greater are the chances for nonlinear behavior to arise. Although steady-state multiplicity region lies in a narrow range of residence times, the simulation results have shown that impurities in the feed may widen this region. As far as theoretical future work is concerned, continuation on other process parameters (e.g. recycle ratio) may help to improve the understanding of the reactor behavior. Two-parameter continuation procedures may also help to classify the reactor parametric space. At the moment, traveling waves around the reactor is another issue under consideration. Analyzing this reactor behavior may explain some of the observed phenomena at low recycle ratios.

7. ACKNOWLEDGMENTS

The authors would like to thank Conselho Nacional de Desenvolvimento Científico e Tecnológico (CNPQ – Brazil) for supporting P. A. Melo's staying in Madison, WI. The authors are also grateful to the industrial sponsors of the University of Wisconsin Polymerization Reaction Engineering Laboratory (UWPREL) and also FAPERJ's Grant #E26/150.970-99, for supporting this research.

8. NOTATION

B	reactor adiabatic temperature rise
Da	Dankӧhler number
f_c	feed molar ratio
Pe_h	heat Peclet number
Pe_m	mass Peclet number
Q	volumetric flow rate
Rec	recycle ratio
t	dimensionless time
U	heat transfer coefficient
y	dimensionless concentration
z	dimensionless axial coordinate
α	modified recycle ratio ($\alpha = \frac{Rec}{Rec+1}$)
β	dimensionless heat transfer coefficient
θ	dimensionless temperature
$\Re$	dimensionless reaction rate
τ	reactor residence time

Subscripts, superscripts

1	tubular zone 1
2	tubular zone 2
Feed	feed conditions

9. REFERENCES

Belkhiria, S., Meyer, T. and Renken, A. (1994), Styrene maleic anhydride copolymerization in a recycle tubular reactor: reactor stability and product quality, *Chem. Eng. Sci.*, **49**, 4981-4990.

Doedel, E.J., Champneys. A.R., Fairgrieve, T.F., Kuznetsov, Y.A., Sandstede, B. and Wang, X. (1997), AUTO97: Continuation and bifurcation software for ordinary differential equations. Technical Report, Computational Mathematics Laboratory, Concordia University.

Fleury, P.A. and Renken, A. (1992), Solution polymerization of methyl-methacrylate at high conversion in a recycle tubular reactor, *Chem. Eng. Sci.*, **47**, 2597-2602.

Hamer, J.W. (1983), Solution polymerization in continuous stirred tank reactors and tubular reactors. Ph.D.'s thesis, University of Wisconsin, Madison.

Hyanek, I., Zacca, J., Teymour, F. and Ray, W.H. (1995), Dynamics and stability of polymerization process flowsheets, *Ind. Eng. Chem. Res.*, **34**, 3872-3877.

Petzold, L.R. (1982), A description of DDASSL: a differential/algebraic system solver. Technical Report SAND82-8637, Sandia National Laboratories.

Teymour, F. (1989), The dynamic behavior of free-radical solution polymerization in a continuous stirred tank reactor. Ph.D.'s thesis, University of Wisconsin, Madison.

Zacca, J.J. (1991), Mathematical modelling of the liquid phase polymerization in loop reactors. Master.'s thesis, University of Wisconsin, Madison.